Polymer 50 (2009) 6065–6075

Contents lists available at ScienceDirect

Polymer

journal homepage: www.elsevier.com/locate/polymer

Characterization of cross-linked polyampholytic gelatin hydrogels through the rubber elasticity and thermodynamic swelling theories

Julio A. Deiber [a,*], Mariel L. Ottone [a], María V. Piaggio [b], Marta B. Peirotti [a]

[a] Instituto de Desarrollo Tecnológico para la Industria Química (INTEC), Universidad Nacional del Litoral (UNL), Consejo Nacional de Investigaciones Científicas y Técnicas (CONICET), Güemes 3450, S3000GLN, Santa Fe, Argentina
[b] Cátedra de Bioquímica Básica de Macromoléculas, Facultad de Bioquímica y Ciencias Biológicas, UNL, Paraje El Pozo, CC 242, S3000ZAA, Santa Fe, Argentina

ARTICLE INFO

Article history:
Received 5 August 2009
Received in revised form
16 October 2009
Accepted 19 October 2009
Available online 25 October 2009

Keywords:
Cross-linked gelatin hydrogels
Mechanical-Electrokinetic properties
Network mesh size

ABSTRACT

A new approach is proposed to characterize polyampholytic gelatin hydrogels, cross-linked covalently with glutaraldehyde. An experimental methodology involving simple mechanical extension and compression and equilibrium swelling tests is developed to estimate relevant microstructural parameters and electrokinetic properties of this type of hydrogel, for different cross-linker to gelatin mass ratios. The polyampholytic cross-linked matrices are studied here in the framework of the rubber elasticity and thermodynamic swelling theories. The main purposes of this work are the estimations of average mesh size and toughness of the swollen hydrogels, and the determination of the feasibility of polyion complexation between cross-linked gelatin chains and bioactive macromolecules to be delivered through hydrogel biodegradation.

1. Introduction

Gelatin is a biopolymer widely used in practical applications of the pharmaceutical, biotechnological and food industries. It is composed of polydisperse polypeptides obtained through either acid, alkaline and mixed processes from different collagen types present in natural sources, like bovine hides and pig and fish skins [1–3]. In this regard, natural polypeptides are polyampholytic macromolecules containing both positive and negative charges. In dilute aqueous solution, these chains present a competition between repulsion electrostatic forces that tend to open chain domains and fluctuation-induced electrostatic attractions promoting chain collapses (see, for instance [4–12], describing basic conformational properties of generic polyampholytes through scaling analyses and molecular dynamic simulations). In this context, it was found that polyampholytes may adopt different conformations depending mainly on the excess and total charge fractions of chains, at a given pH and ionic strength I. These aspects are even more important for situations where the solvent is low in salt contain. It is also clear that at extreme pH values and rather low I, a change of polypeptide behaviors from polyampholytic to polyelectrolytic regimes is expected. This aspect depends, in part, on the polypeptide amino acid sequence determining the isoelectrical point pI. The description and analysis of these regimes for generic charged macromolecules may be found, for example, in [12–15] and citations therein. In particular, the polyelectrolyte regime involves chains with high excess and rather low total charge fractions [12]. Therefore, for the purposes of the present work, it is important to visualize the differences between polyampholytic and polyelectrolytic chains forming hydrogels, mainly in relation to their possible conformations and electrokinetic properties in the cross-linked network. From the available literature, it is clear that most of previous studies concerning characterization methods of charged and covalently cross-linked hydrogels were developed for the case where the basic network was composed of synthetic polyelectrolytic chains (see, for example [16–30], and citations therein). Thus, synthetic polyampholytic hydrogels were much less studied (see [24,31,32] where the effect of added salt was considered in detail). At present, applications of natural polyampholytic hydrogels, like the gelatin-case, are becoming more important [33–41] and hence new quantitative characterization methods for these covalently cross-linked hydrogels are still required. One concludes that they must be proposed considering appropriate methodological innovations starting from previous works developed for synthetic polyelectrolytic and polyampholytic hydrogels. This is the proposal of the present work.

Gelatin chains in solution may be covalently cross-linked to form matrices capable of swelling in the presence of aqueous solutions, forming what is usually designated gelatin hydrogels. The chemical cross-linkers used may be either relatively small

* Corresponding author. Tel.: +54 0342 4559175/77; fax: +54 0342 4550944.
E-mail address: treoflu@santafe-conicet.gov.ar (J.A. Deiber).

0032-3861/$ – see front matter © 2009 Elsevier Ltd. All rights reserved.
doi:10.1016/j.polymer.2009.10.046

bifunctional molecules or polyfunctional macromolecules like, for instance, glutaraldehyde (GTA), carbodiimide, genipin, polyvinylalcohol, etc. [42–47] which bind either amino or carboxylic residues of polypeptide chains (see also [48] for a revision of hydrogel forming polymers and their cross-linking through other physicochemical mechanisms). Thus the resulting gelatin hydrogel is composed of both chemical and physical cross-links, taking into account that below the temperature gel point, gelatin chains revert partially to the tropocollagenic triple helix, from disordered to rather ordered states, depending on temperature, concentration and rate of cooling [2,3]. This phenomenon occurs usually at around 28 °C, where the coil to helix transition is observed (the transition temperature depends on species sources and protein concentration). The result is that parts of either three chains or two chains in a physical "hair-pin" bond type are stabilized mainly through hydrogen bonds [1–3,49,50], forming thus a basic physical network coupled to the covalent one (Fig. 1).

Although gelatin hydrogels have the advantages of presenting biocompatibility and biodegradability with an innocuous nature response in bio-applications and pharmacological formulations, concerns are mainly in relation to the citotoxiticy produced by the type of cross-linker that could remains in the matrix. In this context, transglutaminase is a feasible alternative [51,52]. Independently from this particular aspect, from a more basic point of view and also for practical reasons, the gelatin matrix in the hydrogel requires to be characterized through several parameters, which in principle define specific formulations and functions of this product. Thus, at present there is consensus that either natural and synthetic electrically charged cross-linked matrices may be characterized basically through both the classical rubber elasticity [53–56] and the thermodynamic swelling [16–32,53,57] theories involving these matrices. Most of these works consider extensive revision of previous results and challenging aspects, which may not be included and discussed in detail here. Therefore, in this context one expects to evaluate the matrix shear elastic modulus G, the average molecular mass M_c of network strands comprised between two consecutive cross-links in chains with number average molecular mass M, the average matrix mesh size ξ and the swelling ratio $Q_e = V_g/V_p$. Here, V_p is the sample volume of the dry polypeptide matrix and V_g is the corresponding equilibrium volume of the swollen matrix after enough contact with a formulated aqueous solution has been achieved. For this last purpose a physiological solution at pH 7 and $I = 150$ mM at 25 °C is used (see also below concerning the importance of the salt content in the solvent used). This is precisely the main interest in the present work by considering a gelatin produced from bovine hides and the classical GTA cross-linker to form gelatin hydrogels. In addition, relevant electrokinetic parameters are estimated, like for instance, the hydrogel electrostatic zeta-potential ζ emerging from a Donnan-type equilibrium between the swollen and charged polypeptide matrix and the surrounding electrolyte solution [17,20,23–25,31,32,53]. Also the average effective or excess charge numbers per chain Z and Z_p are provided, which are defined as the difference between positive and negative charge numbers (also designated excess charge numbers) of chain ionizing groups before and after the cross-linking process, respectively. In this context, the characteristic scales L_1 and L_2, as defined below, are calculated. They indicate the average lengths of confinement in the hydrogel of the M_c-chains and M-chains, respectively. Thus, electrokinetic properties are estimated taking into account those works where the importance of both gelatin isoelectrical point pI and hydrogel electrical charges to immobilize charged bioactive macromolecules via polyion complexation is reported (see for example [33–38,40]).

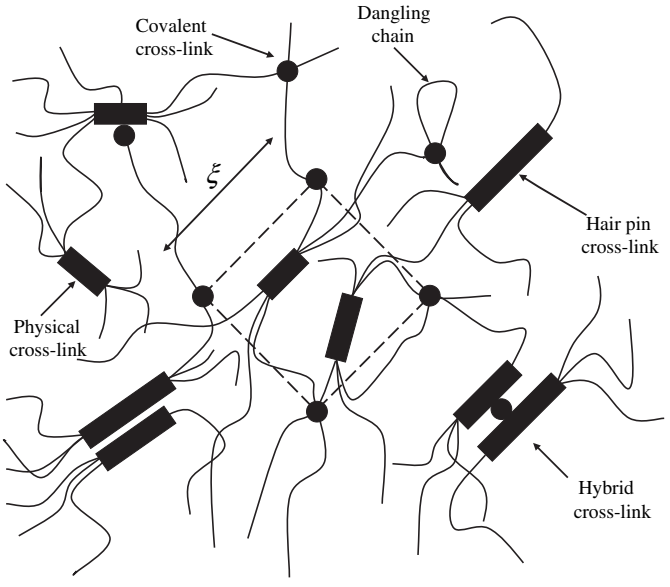

Fig. 1. Scheme illustrating a gelatin hydrogel network. Symbols ● and ▬ refer to covalent and physical cross-links, respectively. Full lines represent gelatin chains and dashed lines delimit an idealized region of the network scaled through the average mesh size.

For this purpose we apply in part basic theories already well established and available in the literature, applicable to both neutral rubbers and electrically charged synthetic matrices covalently cross-linked (for instance, polyelectrolytes of acrylic acid, methacrylic acid, vinil acetate, etc., having mainly one repeating ionizing group, and also polyampholytic copolymers with both positive and negative charges). Therefore, here we extend them to the case of natural polypeptide (polyampholyte) matrices, specifically composed of gelatin chain from bovine hides where ionizing groups are positive Arg, Lys, His and Orn amino acid residues and the terminal amino group, and negative Glu, Asp, Cys and Tyr amino acid residues and the terminal carboxylic group. Therefore different acid dissociation constants must be considered through the corresponding pK_i values, including those of the terminal ionizing groups designated pK_{NH_2} and pK_{COOH} (see Table 1). In this work $i = 1 \ldots N_{AA}$ stands to indicate any type of amino acid residue (ionizing, polar and non-polar) composing the gelatin chain. Therefore, Z and Z_p depend mainly on the pH value of the equilibrating solution used. In these polypeptide chains, Hly (hydroxilysine), Hyp (hydroxiproline) and eventually Orn (Ornitine) may be found. This last one is generated through long time hydrolysis processes transforming part of Arg into Orn [58]. In this context one concludes that the characterization and performance of hydrogels formed with natural polypeptides are different from their counterpart hydrogels composed of synthetic charged homopolymers and copolymers, where the average polymerization index is the relevant parameter. In fact, as pointed out above, the amino acid sequence is also required in the former, at least approximately, as it is described below in Section 2.

In this work, a new approach is proposed in order to interpret the classical experimental methodology involving both simple mechanical extension and compression and equilibrium swelling tests, to characterize relevant microstructural parameters of gelatin hydrogels, for different cross-linker to gelatin mass ratios. In the interplay between tests, one expects also to estimate the value of the Flory–Huggins interaction parameter χ for the pair polypeptide–aqueous solvent, within a consistent physicochemical framework, taking into account the electrolyte solution used as solvent for swelling tests.

Table 1
Amino acid composition of bovine native collagen n_i^b, hydrolyzed collagen n_i^o and gelatin n_i. Also pK_i stands for pK-values of free amino acids residues and amino and carboxylic terminal groups. M_i^r refers to molecular mass of amino acid residues to characterize gelatin Sample B with $M \approx 50$ kDa and $N \approx 547.7$.

Amino acid and terminal groups	pK_i	M_i^r(Da)	n_i^b	n_i^o	n_i
Ala		89	114	114	62.2
Arg	12.48	174	51	51	27.8
Asn		132	16	4.3	2.4
Asp	3.86	133	29	40.7	22.2
Gln		146	48	13	7.1
Glu	4.25	147	25	60	32.8
Gly		75	332	332	181.3
His	6.0	155	4	4	2.2
Hyp		131	104	104	56.8
Hly		162	5	5	2.7
Ile		131	11	11	6
Leu		131	24	24	13.1
Lys	10.53	146	28	28	15.3
Met		149	6	6	3.3
Phe		165	13	13	7.1
Pro		115	115	115	62.8
Ser		105	35	35	19.1
Thr		119	17	17	9.3
Tyr	10.07	181	4	4	2.2
Val		117	22	22	12
Cys	8.33	121			
Trp		204			
Asx		265			
Glx		293			
NH_2-term	9.60	16	1	1	1
COOH-term	2.09	47	1	1	1

Therefore this work is organized as follows. In Section 2, first we describe briefly the relevant characteristics of the average gelatin chain used. They are required as input data in the theoretical framework developed in the following sections. Then the experimental program is briefly presented, where some protocols follow quite closely those already well established by Bigi et al. [59–61] for gelatin hydrogels, mainly in those aspects related to samples preparations, stress and strain responses in simple extension and compression and swelling quantifications. In Section 3 we introduce briefly theoretical and experimental aspects of mechanical tests based mainly on the classical BST rheological model [62] together with useful considerations of the elastic shear modulus in relation to microstructural parameters. In Section 4 the swelling theory of charged matrices is considered to outline a simple strategy that specifically applies to gelatin hydrogels, which is a situation that has been explored a few times within the framework described here (see also [42,45]). Section 5 analyzes and discusses experimental results and numerical evaluations indicating main achievements and limitations of this proposal, which should be considered in future researches of these complex systems. Finally the main conclusions establishing the relevance of characteristic parameters obtained for cross-linked gelatin hydrogels are provided.

2. Materials and methods

2.1. Basic properties and description of the gelatin sample

A gelatin sample (here designated Sample B) obtained from bovine hides and purchased from Sigma Chemical Company, was used in the experimental program involving mechanical and swelling tests ($M \approx 50$ kDa, bloom value of 225 g and pI ≈ 5). Since these gelatin chains are the result of an alkaline process, approximate values of the effective charge number Z per average chain as a function of pH are required in order to estimate the hydrolysis suffered by the amino acid sequence of the native tropocollagen, which must be compatible with the pI of Sample B. This task is carried out by starting from the average amino acid composition n_i^b of the parent tropocollagen chains (see [3] and Table 1). Here the number of the i-amino acid residues in the hydrolyzed collagen chains based on 1003 residues is designated n_i^o. One should also observe that Asn and Gln are partially converted to Asp and Glu, respectively, introducing thus the possibility of yielding gelatins with different pI according to the degree of conversion obtained in the hydrolysis process applied to the collagenic material. Our calculations (see Eq. (1)) indicate that Sample B has a degree of conversion of around 73%, which is the typical value for pI ≈ 5. Table 1 shows the resulting amino acid composition n_i (number of i-amino acid residues per chain with average molecular mass M, after the hydrolysis process) calculated through $n_i \approx n_i^o N/1003$, where $N = \sum_{i=1}^{N_{AA}} n_i$ is the total number of amino acid residues found in the average gelatin chain. It is also clear that some amount of Arg may be converted to Orn when the hydrolysis process is rather prolonged as pointed out in [58]. Nevertheless, this last conversion may be neglected for the process used in the production of these samples.

The estimation of the average effective charge of gelatin chains is carried out as follows,

$$Z = \frac{1}{\left(1+10^{-(pK_{NH_2}-pH)}\right)} \pm \sum_{i=1}^{N_{AA}} \frac{n_i}{\left(1+10^{\mp(pK_i-pH)}\right)} - \frac{1}{\left(1+10^{+(pK_{COOH}-pH)}\right)} \quad (1)$$

where $\pm$ refers to the acid and basic characteristics of ionizing groups. In Eq. (1) pK_i refers to the i-ionizing group of the corresponding free amino acid [63] (see also Table 1). Thus, small effects associated with the "charge regulation phenomenon" are neglected here. A detailed analysis concerning this phenomenon in polypeptides, and the approximations introduced in the use of Eq. (1), may be found in [64–66]. In addition, based on results reported in Table 1, it is also possible to calculate the average molecular mass $M_m = \sum_{i=1}^{N_{AA}} (n_i M_i^r + 18)/N$ of amino acid residues composing the gelatin sample, where M_i^r is the molecular mass of the i-amino acid residue. Here, water molecules lost by amino acids due to the formation of peptide bonds have been accounted. Therefore for Sample B with $M \approx 50$ kDa, one obtains $M_m \approx 91.3$ Da and consequently $N \approx 547.7$.

For calculations presented below, additional parameters characterizing Sample B are the approximate peptide bond length $L \approx 3.6$ Å, the end-to end distance r expressed $r = \alpha L (NC_N)^{1/2}$ and the gyration radius $s = r/\sqrt{6}$ of the average M-chain in aqueous solution (see also these relations involving the M_c-chain in Section 3). Here C_N is the chain characteristic ratio, and α is the excluded volume parameter which tends to value one when theta-conditions are approximated (see also Section 5 below). These relations are suitable approximations as long as the solvent is relatively high in ionic strength, like the physiological solution used here, where Coulombic screening effects may become important for both electrostatic repulsions and fluctuation-induced attractions [12]. Otherwise, the effect of the excess charge numbers Z and Z_p at pH 7 should be accounted. Thus, to have a value of reference here, we found that the excess charge number Z of gelatin chains of Sample B at pH 7 is approximately -8.87, while the critical excess charge number around which the collapsed conformation starts a destabilization [5–9,12,13] in the absence of salt is $-\sqrt{fN_{AA}} \approx -10$. Here $f \approx 0.188$ is the fraction of total charge per average gelatin chain. In

relation to this aspect, calculations carried out for copolymer synthetic polyampholytic hydrogels in [24,31,32] showed that the effect of the excess charge is relevant for $I < 100$ mM, while for higher values of ionic strength, a polyampholytic swelling transition is observed which is not sensitive to excess charge numbers due to Coulombic screening effects (see also Section 5 for a discussion concerning Z_p and the ionic strength used in this work).

Gelatin samples are cross-linked with GTA (molecular mass $M_b = 100.1$ Da) through the ε–amino groups of Lys and Hly amino acid residues reported in Table 1. The total number of these groups is designated $X = n_{Lys} + n_{Hly}$, and from Table 1, $X = 18$ for Sample B. After a given addition of GTA expressed as the ratio m_b/m_p, where m_b is the mass of GTA used in the cross-linking process and m_p is the mass of gelatin, one may estimate the number of cross-linked sites X_C and the effective number of Lys and Hly remaining in the chain designated X_E. In principle the relation $X_E = X - X_C \approx X \exp(-A\, m_p/m_b)$ is used, where A is a constant evaluated at the critical value $(m_b/m_p)_c$ above which addition of GTA does not produce further cross-links. We found that for GTA of around 1%, or equivalently for $(m_b/m_p)_c \approx 0.2$ (see Section 2.2), the critical mass ratio to saturate the cross-linking process is reached. Thus for $A \approx 15$, around 95% of the total number of available sites for cross-link are converted (see also [42,59], where maximum values of experimental conversions of 95% and 98% are reported, respectively, for different gelatin types). Further, it is also clear that for each GTA concentration, chains have a modified net charge number expressed, $Z_p = Z - X_C$. Here, $Z = -8.87$ for Sample B, as deduced from Eq. (1) and Table 1.

Before ending this section, it is important to point out that quantities like n_i^o, n_i, N, X, X_C and X_E are integer values in order to have physical meanings as number of amino acids residues and sites involved in covalent cross-links. Nevertheless, throughout this work calculations were carried out with their values expressed as real numbers and reported at least with one digit, to obtain thus consistency in number balances and higher precision in the final results (other authors usually report some of these numbers as percentage of the total number of sites available for cross-links).

2.2. Hydrogel preparations

For the purposes of this work gelatin films were prepared with a 5 % w/w gelatin aqueous solution at 25 °C [59]. Thus, the required amount of gelatin powder was dissolved in distilled water at 50 °C for 15 min in 50% of the water required. Then the hydrated slurry was completed with additional water to get a particle suspension with a protein concentration of 5% w/w. The suspension was subject to magnetic stirring by still keeping a constant temperature of 50 °C until the dissolution was achieved (around 45 min were needed). Also, 0.02% of sodium azide was added to prevent bacterial degradations. Solutions were prepared at the beginning of each test to avoid secondary effects in the maturation process. They were also filtered and subject to a fixed protocol for each experiment. Thus gelatin films (strips and disks; see also below) were obtained in Petri dishes by pouring different volumes of gelatin solution to get the desired thicknesses. After evaporation at room temperature and subsequent air drying, the thermo-sensible physical hydrogels were cross-linked with 10 ml of GTA solutions of different concentrations (0.025, 0.125, 025, 0.5 and 1% of GTA, prepared in phosphate buffer at pH 7.4 and $I \approx 23$ mM) for 24 h at room temperature. After washing repeatedly with distilled water and then air drying at room temperature, the gelatin films were ready for further analysis. Therefore, we designate here Hydrogel B the films obtained from Sample B and different GTA concentrations. At this stage by weighing hydrogel films wet and dried, the ratio $Q_o = V_o/V_p$ was determined for each GTA concentration used, where V_o was the volume of the relaxed hydrogel after covalent bonds were formed with GTA (see [16] for an analysis of this aspect) and V_p was the volume of the dried sample (see also Section 2.4).

2.3. Simple extensional and compression mechanical tests

Following the procedure suggested by Bigi et al. [59] for simple extension tests, hydrogel strips 4 cm long (effective testing length) and 1 cm wide were prepared. Optical microscopy was used to determine the average thickness (an average value of 0.135 mm was found). Similarly, hydrogel disks 3.5 mm in average height and 4 cm in average diameter were also prepared for compression (biaxial extension) tests. These Hydrogel B samples were equilibrated in a mixture of water-ethanol in the ratio 2:3 for 72 h to improve their dry deformation by plasticization [59], and still keeping the appropriate strength for testing. Then through the weighing process of strip samples, the ratio $Q_{aw} = V_{aw}/V_p$ was determined, where V_{aw} was the volume of the hydrogel equilibrated with the alcohol–water solution. This ratio must be used below to correct the determination of M_c. The plasticized strips and disks with the alcohol–water solution were tested in simple extension and compression, respectively. A Shimadzu DSS-10 T-S machine was used at an axial velocity of 5 mm/min. Thus, the axial force as a function of time was recorded and the stretch ratios λ (axial and biaxial) in both tests were calculated, for further analysis. True stresses were then evaluated by considering the actual cross sectional area of the sample as a function of the axial testing displacement by assuming isochoric deformations.

2.4. Swelling tests

To study the swelling of Hydrogel B, dried hydrogel strips were immersed in physiological solutions (pH 7 and $I = 150$ mM) until the equilibrium between swollen film and solution was achieved at around 72 h. This condition corresponded to a time independent ratio $Q_e = V_g/V_p$ as a function of immersion time. Here V_g was the volume of the swollen sample once the equilibration was achieved. For this purpose the amount of absorbed water in the hydrogel was determined by difference of weights between dried and wet strips [59]. Similar procedures were used to determine Q_{aw} and Q_o (see Table 2). For these purposes, the specific volumes of gelatin and solvent were used (0.73 and 1 cm^3/g, respectively).

3. Stress and strain responses of the gelatin hydrogel

From the classical rubber elasticity theory (see [53,56] and citations therein) three basic responses of an elastomeric material under simple extension are usually found, mainly at low rates of extension. Thus, for low strains the linear elastic response is present, which allows one to estimate the shear elastic modulus. This modulus is a function of the average strand molar mass M_c, and may be also interpreted through different ideal frameworks involving, for instance, the two asymptotic responses described

Table 2
Numerical values of relevant parameters resulting from the rheological characterization of Hydrogel B in simple extension and the swelling experiments.

GTA (%)	$\frac{m_b}{m_p}$	G (MPa)	n	Q_{aw}	Q_o	M_c (Da)	Q_e	ξ (Å)	ξ_s (Å)
0.025	0.005	0.12	4.0	4.71	5.33	13008	5.99	126	73
0.125	0.025	0.17	7.0	3.42	3.59	10999	4.38	105	61
0.25	0.05	0.24	8.0	3.38	3.57	8924	3.92	91	53
0.5	0.1	0.36	9.2	3.06	3.53	6609	3.37	74	43
1.0	0.2	0.58	10.7	3.07	3.37	4620	3.28	62	36

through the affine and phantom network models (see a detailed analysis in Mark and Erman [56], and citations therein). At intermediate strains a softening response may be observed, which is due to entanglements. This zone has been deeply studied and discussed in the literature after the Mooney-Rivlin equation was presented (see, for instance [56,67],). Finally at relatively high strains, cross-linked chains reach their maximum stretching to get a rather sharp hardening zone before breaking. As long as the elasticity of gelatin hydrogels in simple extension is concerned, a sequence of interesting works by Bigi et al. [59], involving hydrogels composed of gelatins from pig skins, permitted us to observe that the gelatin matrices cross-linked with different concentrations of GTA and hydrated with alcohol–water solutions, did not show the softening intermediate response. From our experiments in simple extension, where a gelatin from bovine hide was used to obtain Hydrogel B strips, once more the effect of entanglements were not evident, as shown by the symbols indicating experimental points of stress difference versus stretch ratio in Fig. 2. This aspect suggests one to search a rheological constitutive equation appropriate for this particular hydrogel response. Therefore, among several models available in the literature, in this work the two-parameter BST constitutive equation, valid for isochoric deformations, is proposed. The differences between pairs of stresses σ_i and σ_j are expressed [62],

$$\sigma = \sigma_i - \sigma_j = \frac{2G}{n}\left(\lambda_i^n - \lambda_j^n\right) \tag{2}$$

for i and j taking any value from 1 to 3, where $I = (\lambda_1^n + \lambda_2^n + \lambda_3^n - 3)/n$ is the first invariant of the Seth deformation field [68] defined as $E_i = (\lambda_i^n - 1)/n$, in terms of the principal stretch ratios λ_i, for $i = 1, 2, 3$. Also G is the constant shear modulus and $n > 0$ is the coefficient of the strain measure. Since this model has associated the strain energy density function $U = 2GI/n$, it is simple to find the Hencky hydrogel toughness T_H in simple extension by evaluating this last equation through the corresponding fracture stretch ratio λ_F. In fact, the relations $\lambda_1 = \lambda$, $\lambda_2 = 1/\sqrt{\lambda}$, $\lambda_3 = 1/\sqrt{\lambda}$ at $\lambda \approx \lambda_F$ apply and the strain invariant at fracture is $I_F = (\lambda_F^n + 2\lambda_F^{-n/2} - 3)/n$ (lower index F indicates fracture throughout this work). From these results T_H is simply,

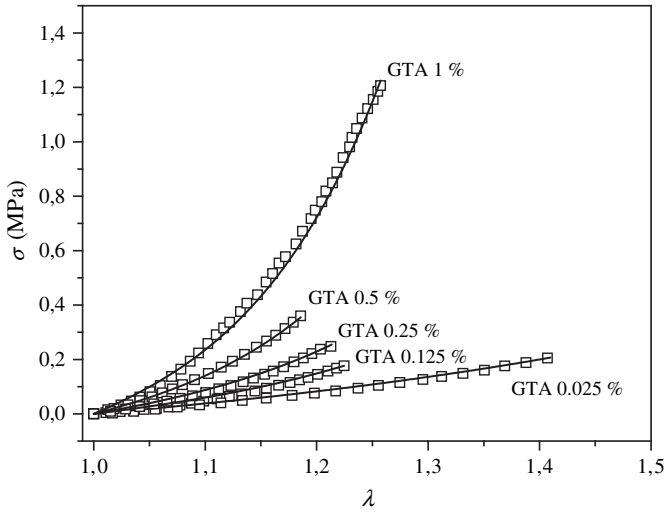

Fig. 2. Stress difference $\sigma = \sigma_1 - \sigma_2$ as a function of stretch ratio λ at 5 mm/min, for Hydrogel B processed with different concentrations of GTA solutions. Symbols refer to experimental data in simple extension. Full lines refer to fittings of experimental data with $\sigma = 2G(\lambda^n - \lambda^{-n/2})/n$ derived from Eq. (2).

$$T_H = \int_0^{\ln\lambda_F} \sigma \, d\ln\lambda = U(I_F) = 2\frac{G}{n} I_F \tag{3}$$

where the Hencky strain is $\varepsilon_H = \ln\lambda$ and $\sigma = \lambda\partial U/\partial\lambda$. It is then clear that T_H may be evaluated directly from experimental λ_F, once the two parameters of the BST model are available at each m_b/m_p.

The BST model is used below to fit experimental data in simple extension of Hydrogel B in order to determine G and n. Then these parameter values and the tensorial structure of Eq. (2) is used to predict the Hydrogel B response in compression or biaxial extension, where $\lambda_1 = \lambda_2 = \lambda$, and $\lambda_3 = 1/\lambda^2$. These results are compared with experimental data obtained as described in Section 2. Here it is evident the importance of using a non linear rheological model to obtain more precisely the value of G from a wide range of strains including the stress hardening response, and also by correlating quite simply the gelatin hydrogel toughness with rheological parameters G and n.

Once G is evaluated at a concentration of the cross-linking agent, this modulus may be correlated with the principal parameters of the hydrogel microstructure like average molecular masses M_c and M, and protein density ρ_p. Thus, by following the classical rubber elasticity theory [53] one expresses, as a first approximation,

$$G = \frac{\rho_p RT}{M_c}\left(1 - \frac{2M_c}{M}\right)\left(\frac{Q_{aw}}{Q_o}\right)^{1/3} \tag{4}$$

where the hydration of gelatin hydrogel with the alcohol–water solution is accounted having as reference the hydration of the relaxed matrix [16]. Also a correction due to terminal ends (non active strands) is introduced in Eq. (4) through the factor $(1 - 2M_c/M)$.

In relation to Eq. (4), it is appropriate to point out here that this expression for G in terms of microstructural parameters involves hypotheses. Thus from the classical rubber elasticity theory this expression is derived by assuming a Gaussian statistic of strands [53] (see also Section 4 below) to end up with a shear modulus proportional to the cross-link density. The particular application of this result to gelatin hydrogels implies that the nature of these cross-links may be covalent, physical and eventually electrostatic (see for instance the descriptions of electrostatic fluctuation-induced attraction forces in [12], and the tropocollagen reversion of gelatin chains to form physical cross-link in [1–3,49,50]). Throughout this work we consider the presence mainly of the two first types, while those of electrostatic nature are neglected taking into account two physical aspects. One considers the fact that cross-linked gelatin chains at pH 7 have a negative excess charge capable to provoke a rather repulsive force between strands impeding the presence of temporarily electrostatic attraction cross-links. The other is that swelling experiments in this work are carried out at $I = 150$ mM, what indicates that Coulombic screening effects occur for both electrostatic fluctuation-induced attractions and repulsion forces (see also the effect of salt in synthetic polyampholytic hydrogels in [31,32]). Thus in this physicochemical framework one expects that Eq. (4) applies approximately by considering mainly chemical and physical cross-links only, and leaving out, as a first approximation, the possibility of additional cross-links from electrical origin (see also Section 5). A detailed analysis of the shear modulus of polyelectrolytic networks is presented in [69] showing, for instance, the associated and complex interplay between charges and salt concentration.

For the swelling protocol used here, it is then clear that when experimental data G, Q_o and Q_{aw} are available, the estimation of M_c from Eq. (4) becomes useful. In fact, the number of total active cross-links per gelatin chain (either physical and covalent) is $(M/M_c - 1)$, while the corresponding number of active strands is

$(M/M_c)(1-2M_c/M)$. Further, M_c is quite useful to estimate the average mesh size ξ in the swollen state, as it has been already suggested in the literature [30,42,45]. Here we use an average mesh size defined as $2\xi/(r_c+s_c) = Q_e^{1/3}$, where r_c and s_c are the end-to-end distance and gyration radii for the M_c-chain. We adopt this definition taking into account that the pair of consecutive cross-links associated with the M_c-chain biases the freely jointed chain statistics of r_c (see discussion in Section 5). Also, as a first approximation, a basic ideal strand having M_c/M_m peptide bonds is considered. Therefore, the average mesh size near theta-conditions is,

$$\xi \approx 0.704 L (C_N M_c/M_m)^{1/2} Q_e^{1/3} \tag{5}$$

where $C_N \approx 5.3$, as a first approximation. This value is estimated for rather short polypeptide chains [70]. In general, it is known that the presence of high content of Gly (33%), Pro (11%) and Hyp (10%) lower the chain characteristic ratio by increasing chain flexibility and also by changing the chain direction through the *cis*-form.

4. Swelling of gelatin hydrogels

A polyampholytic gelatin hydrogel cross-linked with GTA presents a network that contains positive and negative ionizing groups. This network in contact with the physiological solution (pH 7 and $I = 150$ mM) reaches a thermodynamic equilibrium after the exchange of free ions and solvent, resulting thus a swollen network. This situation between the swollen hydrogel and the surrounding bath is usually described as a Donnan equilibrium where the biopolymer network acts as its own membrane [18,24,25,31,32,53] thus preventing the diffusion of the attached ionizing groups toward the solution bath. Consequently, the study of the thermodynamic equilibrium between hydrogel and physiological solution requires the knowledge of the change of total free energy involved in the mixing of dry hydrogel and formulated solution. The total free energy change is decomposed into three parts associated with the free energy of mixing ΔF_S between gelatin and solvent, the change of elastic free energy ΔF_E required to form the deformed network, and the change of the free energy of mixing ΔF_I in the network and the solution bath associated with mobile ions and solvent. It is relevant to indicate here that the swelling of neutral network involves ΔF_S and ΔF_E only (thus solvent chemical potentials in the network and in the bath are equals [53,71]), while polyelectrolytic and polyampholytic networks require also the consideration of ΔF_I owing the presence of electrical charges in the network strands. In this context of analysis several hypotheses are introduced [18,24,25,31,32,53]. Thus the network is amorphous and the deformation process during swelling is isotropic without significant change in the network internal energy (entropic deformation prevails). Further there are not individual biopolymer molecules unattached from the network. Another approximation is that the swollen hydrogel forms roughly a dilute solution (see also corrections in [31,32]). This hypothesis justifies that the total free energy may be expressed as the sum of the basic free energy changes indicated above [53]. Therefore, in this framework, one may use approximate expressions of the chemical potential of ionic species in terms of concentrations. From the Flory–Huggins lattice theory (see also details in [18,53]) the change in free energy of mixing between gelatin and solvent is,

$$\Delta F_S = k_B T (n_1 \ln(1-\nu_2) + \chi\, n_1 \nu_2) \tag{6}$$

where n_1 is the number of solvent molecules in the network, k_B is the Boltzmann constant, T is the absolute temperature and $\nu_2 = 1/Q_e$ is the volume fraction of biopolymer in the swollen network. In Eq. (6), the number concentration of gelatin chains n_2 is zero [53] and hence the corresponding biopolymer volume fraction $\nu_2 = \sum_{i=1}^{N_i} \nu_i$ involving the gelatin polydispersity has not effect on ΔF_S, as long as network defects are neglected [72] (ν_i refers to the volume fraction of the i-chain having molecular mass M_i). Here $i = 1 \ldots N_I$ refers to mobile ions Na^+, H^+, Cl^- and HO^- only. It should be observed that the lattice theory used in the deduction of Eq. (6) considered a uniform cell volume [53], and hence this theoretical hypothesis is less applicable to the particular case of amino acids residues of polypeptide chains.

From the affine network model the change of the network elastic free energy is [18,53],

$$\Delta F_E = k_B T \nu_e \left(3\lambda_s^2 - 3 - \lambda_s^3\right) \tag{7}$$

where ν_e is the effective number of strands in the network and $\lambda_s = Q_e/Q_o$ is the isotropic stretch ratio of the swollen network referred to the unrelaxed state after the cross-linking process ([16,18]). For highly cross-linked hydrogels, non Gaussian effects in chain stretching require an extended version of Eq. (7) [25,73–75].

The change of free energy of mixing associated with free ions and solvent is [53],

$$\Delta F_I = \sum_{i=1}^{N} \left\{ \left(\mu_i^* - \mu_i^o\right) n_i^* + \left(\mu_i^\infty - \mu_i^o\right) n_i^\infty \right\} \tag{8}$$

where $i = 1 \ldots N$ refers to solvent and mobile ions Na^+, H^+, Cl^- and HO^-, and n_i stand for molecule numbers of these species. In Eq. (8), μ_i^o are the chemical potentials of pure species, while μ_i^* and μ_i^∞ are the chemical potentials of species evaluated in the hydrogel and in the equilibrating solution, respectively.

Therefore the condition for solvent equilibrium between swollen hydrogel and solution implies the minimization of the total free energy $\Delta F_S + \Delta F_E + \Delta F_I$. Thus this expression is differentiated with respect to solvent molecule number n_1^* and the result is equated to zero (Gibbs–Duhem equation and $dn_1^\infty = -dn_1^*$ is used in the algebraic process). Then after multiplying by the Avogadro constant N_A, normalizing with the solvent molar volume $V_1 \approx 18\ cm^3/mol$, and introducing approximations related to the dilution hypothesis, the resulting equation expresses the equilibration of three osmotic pressures. They are useful for the estimations of the relevant electrokinetic properties indicated in Section 1. One is the osmotic pressure P_I associated with ΔF_I, involving the exchange of solvent and mobile ions between both phases, taking into account that each gelatin chain in the hydrogel has an effective electrical charge Z_p, at a given value of pH and I, due to ionizing groups as described in Section 2. The other two osmotic pressures P_E and P_S involve the elastic resistance to swelling of the hydrogel macromolecular network, and the mixing between gelatin and solvent, respectively. Thus they are associated with ΔF_E and ΔF_S. It is then clear that within the general framework described above, we extend briefly previous studies to the case of polyampholytic gelatin hydrogels placing emphasis in the estimation of P_I through a practical and simple expression (see also [17,31,32]). Here, as a first approximation, the excess osmotic pressure corrections in ΔF_I and P_I for polyampholytic hydrogels are neglected, taking into account that for characterization purposes only, one should need a simple problem. Also, since the ionic strength used here is still low enough, the hydrogel swelling transition for very high salt content may be also neglected. In this regard, for $200 < I < 1000$ mM, where the screening polyampholytic regime with excluded volume effects appears in synthetic polyampholytic hydrogels, English et al. [32] proposed a second order correction for P_I through Mayer's theory. This more complex model provided good qualitative swelling predictions

when a comparison with experimental results was carried out at very high salt concentrations. These aspects would require further research for complex natural polyampholytic hydrogels in solutions with very high salt content.

Therefore, following Flory [53] and modifications by Peppas and Merril [16], from Eq. (7) we obtain,

$$P_E = \frac{RT}{\bar{v}M_cQ_o}\left\{1-\frac{2M_c}{M}\right\}\left\{\left(\frac{Q_o}{Q_e}\right)^{1/3}-\frac{Q_o}{2Q_e}\right\} \quad (9)$$

where $\bar{v}$ is the specific volume of gelatin chains and $R = k_BN_A$ is the gas constant. It should be observed that in Eq. (9) the number concentration of effective strands in the network is expressed in relation to the dry network volume V_p as follows [18],

$$\frac{\nu_e}{V_p} = \frac{1}{\bar{v}M_c}\left\{1-\frac{2M_c}{M}\right\} \quad (10)$$

Further, since our calculations show that gelatin hydrogels cannot exceeds a GTA cross-linker concentration higher than 1% leaving a high enough number of amino acids per strand (M_c/M_m higher than 50) we found that Eq. (9) is sufficiently accurate in relation to other improved versions involving non Gaussian chain stretching responses [25,73–75]. Also, from Eq. (6), one obtains,

$$P_S = \frac{RT}{V_1}\left\{\ln\left(1-\frac{1}{Q_e}\right)+\frac{1}{Q_e}+\frac{\chi}{Q_e^2}\right\} \quad (11)$$

After considering that the osmotic coefficient is around unity under dilute conditions (see, for instance [13], for an analysis of this coefficient in polyelectrolytic network without added salt) the following thermodynamic expression derived from Eq. (8) applies,

$$P_I = -RT\sum_{i=1}^{N_I}\left(C_i^* - C_i^\infty\right) \quad (12)$$

where C_i^* are the concentrations of mobile ions within the hydrogels and C_i^∞ are the concentrations of the same ions in the equilibrating solution far away from the hydrogel surface, where the electrical double layer yields an electrical zeta-potential ζ. As long as the expression for P_I is concerned, we have decided to go back to Flory's works (see [53] and citations therein) and to follow the proposal of using the electrical zeta-potential of the hydrogel surface as the controlling parameter of the Donnan-type equilibrium generated between polymeric matrix and electrolyte solution (see also [17,20,23,24,31,32]). Thus, it should be observed that the ratio of these concentrations may be expressed,

$$C_i^* \approx C_i^\infty \exp(-ez_i\zeta/k_BT) \quad (13)$$

where e is the elementary charge and z_i is the charge number of i-ion. When this expression is replaced into Eq. (12), one readily obtains,

$$P_I = RT\sum_{i=1}^{N_I} C_i^\infty\{\exp(-ez_i\zeta/k_BT)-1\} \quad (14)$$

Thus at pI of the gelatin matrix (which is not necessarily the same pI as that of the gelatin chain before cross-linking; see Section 5) $P_I = 0$ because ζ=0 and $Z_p = 0$. It is also clear that as long as ζ is known the effective hydrogel charge number Z_p may be obtained from the condition of electro-neutrality in both phases far from the interface as follows,

$$\sum_{i=1}^{N_I} C_i^\infty\{\exp-(ez_i\zeta/k_BT)\} + Z_pC_p = 0 \quad (15)$$

where $C_p = 1/(\bar{v}MQ_e)$ is the molar concentration of gelatin in the swollen hydrogel. Consequently at equilibrium, the resulting balance equation involving osmotic pressures is,

$$P_E + P_S + P_I = 0 \quad (16)$$

Both Eqs. (15) and (16) are subject to the constrain,

$$X_E \approx X\exp(-Am_b/m_p) \quad (17)$$

where an approximate maximum conversion of 95 % was considered, as discussed in Section 2. Once experimental values Q_e and M_c at each GTA concentration are available, Eqs. (15) to (17) are solved simultaneously to find χ, ζ and Z_p through an iterative procedure involving trial electrical zeta-potentials until consistency with Eq. (17) is achieved. Previous relations, $Z_p = Z - X_C$ and $X_E = X - X_C$, are useful for this purpose (see Section 2).

Once the hydrogel electrical zeta-potential is known from the numerical procedure indicated briefly above, the electrical charge density q is evaluated as follows [76],

$$q = 2(2\varepsilon k_BTn^\infty)^{1/2}\sinh\left(\frac{eZ_p\zeta}{2k_BT}\right) \quad (18)$$

Further $q = eZ_p/(A_oQ_e^{2/3})$, where the characteristic area A_o covering the confinement of the cross-linked M-chain is corrected with the factor $Q_e^{2/3}$ as a consequence of hydrogel swelling. Therefore, the evaluation of A_o allows one to define the characteristic electrokinetic lengths $L_1 \approx \sqrt{A_oQ_e^{2/3}M_c/M}$ and $L_2 \approx \sqrt{A_oQ_e^{2/3}}$ associated with the confinements of the M_c-chain and M-chains in the hydrogel, respectively (see for instance [12,77] for scale analyses in general involving polyampholytic and polyelectrolytic macromolecules).

5. Results and discussion

Fig. 2 shows the fitting of Eq. (2) to experimental stress difference σ as a function of stretch ratio λ, for the simple extension test of Hydrogel B strips. An average relative error of around 3% was obtained, allowing one a neat determination of G and n, as reported in Table 2. It is clear that although Eq. (4) is corrected due to relative swelling and the existence of non active terminal strands, other network imperfections like dangling loops cannot be described here (see Fig. 1). Thus the prediction of M_c must be associated with active strands and cross-links only. This aspect implies that estimations are carried out within a rather ideal framework in order to obtain approximate average values of topological parameters of this complex system. Nevertheless, even within this type of quantifications, one expects these results to be consistent with those found from swelling thermodynamic considerations as described below.

From Table 2, it is readily found that $G = 0.115 + 2.354\ m_b/m_p$ (MPa) with a correlation coefficient $r^2 \approx 0.9982$. Thus around 19.6% of the value of G at 1% GTA may be associated with physical cross-links taking into account that for $m_b/m_p = 0$ the shear modulus is not null. In relation to this last result, Hydrogel B swollen with the alcohol–water solution does not show a relevant effect of entanglements at intermediate deformations as discussed in Section 3. Only a weak onset of this response for 1 % of GTA is almost visualized in Fig. 2, perhaps due to physical cross-link disruptions at this high level of GTA concentration, thus promoting some entanglement formation. Therefore the value $G \approx 0.115$ MPa

at zero concentration of GTA could be attributed mainly to physical cross-links. In this context M_c is considered an effective average molecular mass between two consecutive cross-links, taking into account that in some places they may differ in nature. In fact physical cross-links involve a rather extended zone of triple helix formed due to partial tropocollagen reversion (Fig. 1).

Within the rheological framework and with the parameters of the BST model, the Hencky toughness T_H of Hydrogel B is evaluated through Eq. (3) and results are illustrated in Fig. 3. One observes at one extreme that Hydrogel B becomes tougher as the number of covalent cross-links increases generating the higher stresses for fracture. This result indicates that at high GTA concentration the average mesh size becomes small enough to have a reduced effect as an initiating "crack" for material failure, generating thus the higher tensions at fracture. Further, it is also observed a smaller relative increment of toughness at the lower extreme of GTA concentrations, where the Hydrogel B presents a low shear modulus, allowing the higher deformation at fracture for this situation.

To exploit further the characterization of Hydrogel B through the BST model, we have evaluated experimentally the fracture invariant I_F in simple extension and compression. In this regard, Table 3 shows that while the fracture stretch ratios of these tests are quite different, as expected in general, the values of the corresponding fracture invariants are approximately equal, at each GTA concentration. Small experimental differences in I_F may be associated with the difficulty found in the manipulation of many strips and disks prepared for these tests, which in addition have different dimensions and shapes producing a rather uneven cross-linking process. For this type of material, the experimental results presented here suggest that I_F is approximately preserved for these two types of deformations tested, and possible for other simple mechanical deformations. Therefore, although this qualitative feature shall not be considered a general criterion for hydrogel fracture, in principle, it may be useful for applying the tensorial structure of Eq. (2) in order to describe approximately other deformation tests with the values of parameters G and n reported in Table 2. In this framework, for instance, Eq. (2) predicts qualitatively experimental stress difference σ as a function of stretch ratio λ for the compression test of Hydrogel B disks (see Fig. 4). Through these qualitative considerations, in general one concludes that Hydrogel B is a weaker material mainly for shear and constant stretch rate deformations and tougher mainly at high and much less at low GTA concentrations. These calculations also allow one an estimation of the shear and stretch ratio ranges where approximate stress values may be estimated for different well known deformation tests. They may be selected to study hydrogel mechanical responses under different manipulations in practical uses.

Table 3
Experimental values of fracture stretch ratios and strain invariant for the simple extension and compression tests of Hydrogel B at different GTA concentrations. Seth fracture strain invariants are $I = (\lambda_F^n + 2\lambda_F^{-n/2} - 3)/n$ for simple extension and $I = (\lambda_F^{-2n} + 2\lambda_F^n - 3)/n$ for compression or biaxial extension. Values of n are taken from Table 1.

GTA (%)	Compression		Simple Extension	
	λ_F	I_F (λ_F)	λ_F	I_F (λ_F)
1	1.18	0.79	1.26	0.86
0.5	1.12	0.30	1.19	0.29
0.25	1.14	0.35	1.21	0.33
0.125	1.15	0.37	1.22	0.30
0.025	1.25	0.50	1.41	0.48

Before ending this part of the discussion, several correlations emerging from the experimental data are useful for estimating the hydrogel toughness quite simply. For instance the correlation $n = 100\sqrt{m_b/m_p}/(7\sqrt{m_b/m_p} + 1.3)$ with $r^2 \approx 0.9976$ is useful to estimate n from the concentration of the GTA solution used, when the methodology proposed in Section 2.2 for Hydrogel B preparations is followed. Further, without the use of rheological data G and n, the following correlation may be used directly to obtain $M_c 10^{-3} = 3.9 + 9.7exp(-13\ \ m_b/m_p)$ with $r^2 \approx 0.9997$ for the estimation of the hydrogel average mesh size through Eq. (5) at each value of Q_e. On the other hand, Table 2 reports experimental values of Q_{aw} and Q_o used in Eq. (4) to evaluate M_c, as well as values of Q_e, which through Eq. (5) provide an estimation of the average mesh size ξ of Hydrogel B for different GTA concentrations.

The numerical predictions of the approach proposed here to characterize polyampholytic hydrogels are consistent with physical aspects to be found from elementary consideration of the rubber elasticity theory. Thus increments of the GTA concentrations also increase the number of active strands per chain, and hence generate hydrogels with higher shear moduli, to which lower values of the average molecular mass between two consecutive

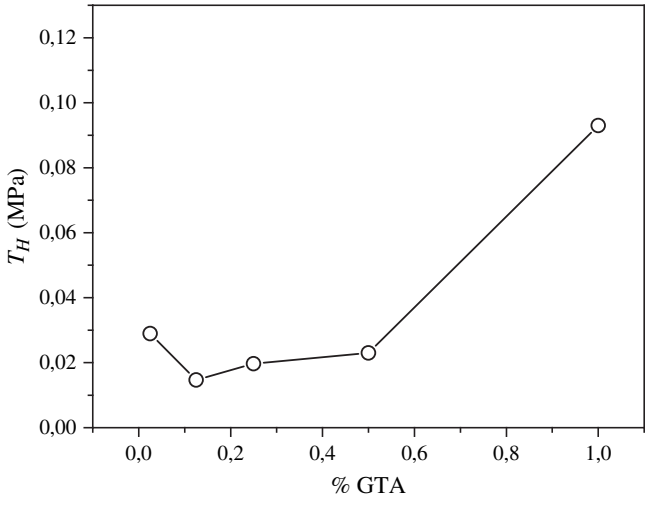

Fig. 3. Hencky Toughness T_H as a function of GTA concentration. Symbols refer to values calculated with Eq. (3) and fracture experimental data from Fig. 2. Full straight lines are traced to visualize the relationship only.

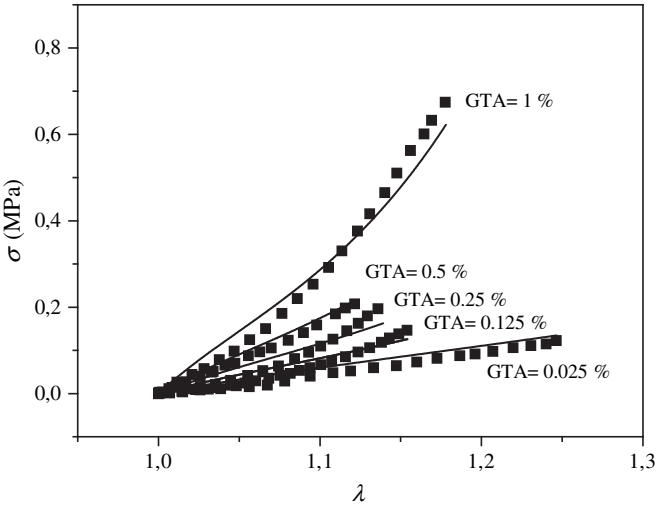

Fig. 4. Stress difference $\sigma = \sigma_1 - \sigma_3$ as a function of stretch ratio λ at 5 mm/min, for Hydrogel B processed with different concentrations of GTA solutions. Symbols refer to experimental data in compression or biaxial extension. Full lines refer to predictions with $\sigma = 2G(\lambda^n - \lambda^{-2n})/n$ derived from Eq. (2).

cross-links M_c correspond, owing to the approximate inverse relationship between these two parameters (see Eq. (4)). Therefore from these results it is also clear that the average mesh size must decrease with increasing GTA concentration as indicated and quantified from Eq. (5). In this sense, although the evaluation of ξ is relevant in relation to the hydrodynamic size and shape of any bioactive macromolecule to be loaded in the hydrogel, we do not have sufficient information concerning electrokinetic properties needed to visualize the viability of the "polyion complexation" phenomenon as described in Section 1 (see, for instance, applications of gelatin hydrogels in [33–38,40]). Thus one requires in addition the electrokinetic characterization of Hydrogel B, here carried out with Eqs. (6)–(18). In fact, these equations can be evaluated with the numerical values reported in Table 2 and following the iterative numerical scheme briefly described in Section 4.

Consequently, Table 4 shows electrokinetic parameters obtained for Hydrogel B. Here one finds that as GTA is included in the hydrogel, the energy of interaction between solvent and the macromolecular matrix becomes a little poorer. This conclusion is validated quantitatively through the estimated numerical values of the Flory–Huggins parameter χ reported in this table (see also [25], for similar calculations). It is also clear that the rather constant values near 1/2 obtained for parameter χ validate the condition $\alpha \approx 1$ introduced as a first approximation in Eq. (4). Furthermore, Table 4 shows that the electrical zeta-potential ζ takes higher negative values as more X-sites are being bonded by the GTA molecules. In fact two positive ionizing Lys or Hly amino acid residues are lost due to the covalent combination with each GTA molecule. This physical aspect may be also visualized with the systematic change to higher negative values of the average effective charge number Z_p of the M-chain for increasing GTA concentrations, after the cross-linking process (Table 4). Consistently with these results, the number of sites converted to cross-links X_C, as deduced from the value Z_p, increases with higher concentration of GTA while the remaining effective sites X_E of Lys and Hly in the hydrogel follow the opposite trend to balance the total sites X available initially when no GTA is added (see Section 2). The evolutions of ζ and Z_p with GTA concentration shown in Table 4 are important to achieve polyion complexation between Hydrogel B and, for instance, a positively charged bioactive macromolecule at a pH around 7. In fact, this phenomenon may be more efficient at high GTA concentrations because higher negative values of hydrogel effective charge (or zeta-potential) opposed to those of the positive macromolecule are quantified here (around a charge number of −26 at 1% GTA against −10 for 0.025% GTA at the lower limit where physical cross-links are relevant). In this sense it is also helpful to remember here that the network average mesh size is smaller at higher values of GTA concentrations, creating thus a situation of compromise between the conditions desired for polyion complexation against those of hindrance associated with the size of the biomacromolecule to be loaded in the hydrogel. It is relevant to point out that basic complexation mechanisms among polyelectrolytes, polyampholytes and uniform charged surfaces have been proposed in the literature [13,78–82]. One aspect of interest to this application involving hydrogels is the fact that even in the case that a polyampholyte has an excess charge number of the same sign as that of a charged surface, a rather open complexation between them is possible [78]. Also, the charge distribution along a random polyampholyte influences its complexation with a polyelectrolyte in dilute and semi dilute solutions [13,82] (the polarization-induced attraction interactions are important). In relation to the hydrogel system, it was shown [81] that the affinity in the complexation between network and charged macromolecules is significantly affected by slight increases of salt content due to the competition presented by the ions assumed as "mobile" in the Donnan classical theory.

Table 4
Numerical values of parameters resulting from the characterization of Hydrogel B through swelling experiments and the use of Eqs. (6) to (18). Also, $X = 18$, $Z = -8.87$ and $N = 547.7$.

GTA (%)	$\frac{m_b}{m_p}$	χ	ζ (mV)	Z_p	L_1 (Å)	L_2 (Å)	X_C	X_E	$(M/M_c - 1)$
0.025	0.005	0.562	−3.96	−10.17	60	118	1.3	16.7	2.8
0.125	0.025	0.593	−7.66	−14.54	53	113	5.7	12.3	3.5
0.25	0.05	0.609	−10.69	−18.39	47	111	9.5	8.5	4.6
0.5	0.1	0.634	−15.02	−22.86	40	110	14	4	6.6
1.0	0.2	0.639	−17.24	−25.99	33	110	17.1	0.9	9.8

The two characteristic scales L_1 and L_2 of confinement of the M_c-chain and M-chain, respectively, can be evaluated as reported in Table 4. Certainly the average mesh size is practically comprised between L_1 and L_2. Taking into account that ξ is obtained from rheological measurements, this result is quite relevant to verify the consistency of the numerical predictions, within the range of GTA concentrations. Nevertheless when ξ is evaluated with s_c only in Eq. (5), designated ξ_s and reported in Table 2, the resulting average mesh size is closer to L_1 as one would expect. Thus the end-to-end distance of the M_c-chain is biased statistically by its two end cross-links as indicated in Section 2. It is also observed that L_2 is around three times the value of L_1 at 1% GTA (see Table 4). This last result seems to indicate that the M-chain domain at high conversions of covalent cross-links (around 95%) is rather compact, having still a relevant amount of the original triple helix content. Also the size of L_2 observed in Table 4 is quite conservative for different GTA concentrations. In fact, by increasing the cross-linker concentration, the repulsion among chains due to negative charges become higher while the hydrogel swelling ratio is smaller due a decreasing average mesh size, resulting thus insignificant changes of the M-chain confinement. This analysis involving average physical scales is important to be studied in hydrogel characterizations taking into account that the network elasticity and the swelling of the electrically charged matrix are two phenomena strongly coupled through the evolving parameters M_c, χ, ζ and Q_e with changes of GTA concentration. In general, one finds quite realistic numerical results characterizing Hydrogel B from the approach proposed here, despite the complexity presented by polyampholytic matrices, as it is the case of gelatin-GTA hydrogels.

It is also interesting to observe that the approximate excess charge number per hydrogel strand Z_pM_c/M varies from −4.8 to −1.7 as the GTA concentration increases from 0.025 to 1% (see also Table 4), while the approximate critical excess charge number $-\sqrt{f\,M_c/M_m}$ [5–9,12] around which a collapsed conformation of the M_c-chain starts a destabilization in the absence of salt varies from −5.2 to −3.1, respectively. In this context, the approximate values of actual and critical excess charge numbers of strands indicate that the salt ions of the physiological solution used here introduces Coulombic screening effects, as stated above, taking into account the scales values associated with the M_c-chain and M-chain domains in the hydrogel reported in Table 4.

It remains to be analyzed several specific results before ending this section, which are relevant concerning hydrogel characterizations. Although Tables 1–4 are useful mainly to visualize the global response of the hydrogel, they are not enough to quantify separately the number of covalent and physical cross-links when GTA is incorporated. Nevertheless, one may have still an estimate of the importance of covalent cross-links taking into account that in general $X \geq X_C > (M/M_c - 1)$ when GTA becomes higher, until the critical ratio $(m_b/m_p)_c \approx 0.2$ is reached. In fact, interesting is the case where $(m_b/m_p)_c \approx 0.005$ (the lower GTA concentration used; see Table 4) at which this inequality is not satisfied. For this

particular case it is clear that most of the active strands in the rheological test are provided by physical cross-links having the matrix a few covalent cross-links only, as reported in Table 4. In principle we found that the topology of the network formed in Hydrogel B is different from the ideal one, and that a high number of covalent cross-links (around 50%) may be wasted because they do not become active as it is deduced from the relation $X > X_C > (M/M_c - 1)$ as the GTA concentration increases (see data in Table 4). This result also excludes the possibility of the presence of temporarily cross-links of electrostatic origin as discussed above. Thus the assumption of Coulombic screening effects seems to be consistent when Hydrogel B is swollen in the aqueous solvent at pH 7 and $I = 150$ mM.

Certainly the new approach proposed here to characterize the polyampholytic gelatin hydrogel still presents limitations that must be overcome. Several hypotheses were introduced in order to make this approach amenable to semi analytical quantification without entering into rather complex numerical codes. In future researches, the charge regulation phenomenon [64–66] and the excess osmotic pressure corrections [24,31,32] should be considered for a deeper analysis of polyion complexation between hydrogels and bioactive macromolecules involving specific cases of drug release. Further physical scaling laws of chain must be improved by considering non ideal chain effects; for instance, the numerical scheme may include a refined convergence between parameters α and χ. The effect of pH and I changes on the swelling of gelatin hydrogels should be also studied on the base of previous works for hydrogels from synthetic chains [24,25,31,32]. Finally additional experiments evaluating the number of converted sites available for covalent cross-links is desirable, for example, as reported in [42,59], although Eq. (13) is a good approximation for this evaluation.

6. Conclusions

The new approach proposed in this work to characterize gelatin hydrogels, cross-linked covalently with glutaraldehyde, shows that elastic and electrokinetic properties of the resulting network are physically coupled. They depend significantly on the cross-linker to gelatin mass ratio. Thus the estimation of the shear module, average molecular mass between two consecutive cross-links, number of active network strands and average mesh size keep a close relationship with the electrical zeta-potential, effective charge number and confinement domains of characteristic macromolecular chains. This result is helpful to cross-check the consistency of property values obtained in the process of hydrogel characterization. Through the experimental methodology, involving both simple mechanical extension and compression and equilibrium swelling tests, the estimation of microstructural parameters and electrokinetic properties of this type of hydrogel may be readily determined in conjunction with the basic equations of this proposal, in a quite simple numerical procedure. Although cross-linked gelatin hydrogels are more complex than polyelectrolytic and polyampholytic hydrogels composed of cross-linked synthetic polymers, the theoretical framework presented here provides, as a first approximation, a simple characterization. This work allows practical estimations, like the average mesh size and toughness of the swollen polyampholytic gelatin hydrogels, together with the determination of the feasibility of polyion complexation between cross-linked gelatin chains and bioactive macromolecules to be delivered through hydrogel biodegradation. It is also clear that when different types of cross-links may be present in the hydrogel network, the average strand molecular mass should be determined through rheometric tests to avoid rough estimations from stoichiometric considerations. Future researches are expected in order to eliminate some approximations associated with complex electrically charged networks of the rubber elasticity and thermodynamic swelling theories.

Acknowledgements

We thank Prof. Bigi for a valuable comment related to hydrogel swellings in alcohol–water solutions. Authors thank financial aid received from CONICET (PIP-112-200801-01106).

References

[1] Veis A. The macromolecular chemistry of gelatin. 1st ed. New York: Academic Press, Inc.; 1964 (chapter III).
[2] Ledward DA. Gelation of gelatins. In: Mitchell JR, Ledward DA, editors. Functional Properties of food macromolecules. New York: Elsevier Applied Science Publishers; 1986. p. 171–201.
[3] Ledward DA. Gelatin. In: Phillips GO, Williams PA, editors. Hanbook of hydrocolloids. Boston: Woodhead Publishing Limited; 2000. p. 67–86.
[4] Higgs PG, Joanny JF. J Chem Phys 1991;94(2):1543–53.
[5] Kantor Y, Li H, Kardar M. Phys Rev Lett 1992;69(1):61–4.
[6] Kantor Y, Kardar M, Li H. Phys Rev E 1994;49(2):1383–92.
[7] Kantor Y, Kardar M. Phys Rev E 1995;51(2):1299–312.
[8] Kantor Y, Kardar M. Phys Rev E 1995;52(1):835–46.
[9] Dobrynin AV, Rubinstein MJ. Phys. II France 1995;5(5):677–95.
[10] Everaers R, Johner A, Joanny JF. Macromolecules 1997;30(26):8478–98.
[11] Yamakov V, Milchev A, Limbach HJ, Dünweg B, Everaers R. Phys Rev Lett 2000;85(20):4305–8.
[12] Dobrynin AV, Colby RH, Rubinstein M. J Polym Sci Part B Polym Phys 2004;42(19):3513–38.
[13] Dobrynin AV. Curr Opin Colloid Interface Sci 2008;13(6):376–88.
[14] Dobrynin AV, Rubinstein M. Prog Polym Sci 2005;30(11):1049–118.
[15] Liao Q, Dobrynin AV, Rubinstein M. Macromolecules 2006;39(5):1920–38.
[16] Peppas NA, Merril EW. J Polym Sci Part A Polym Chem 1976;14(2):441–57.
[17] Rička J, Tanaka T. Macromolecules 1984;17(12):2916–21.
[18] Brannon-Peppas L, Peppas NA. Chem Eng Sci 1991;46(3):715–22.
[19] Khare AR, Peppas NA. Biomaterials 1995;16(7):559–67.
[20] English AE, Tanaka T, Edelman ER. J Chem Phys 1996;105(23):10606–13.
[21] Ende MTA, Peppas NA. J Appl Polym Sci 1996;59(4):673–85.
[22] Hariharan D, Peppas NA. Polymer 1996;37(1):149–61.
[23] English AE, Tanaka T, Edelman ER. J Chem Phys 1997;107(5):1645–54.
[24] Mafé S, Manzanares JA, English AE, Tanaka T. Phys Rev Lett 1997;79(16):3086–9.
[25] Eichenbaum GM, Kiser PF, Dobrynin AV, Simon SA, Needham D. Macromolecules 1999;32(15):4867–78.
[26] Peppas NA, Bures P, Leobandung W, IchikawaEur H. J Pharm Biopharm 2000;50(1):27–46.
[27] Peppas NA, Huang Y, Torres-Lugo M, Ward JH, Zhang J. Annu Rev Biomed Eng 2000;2(1):9–29.
[28] Metters AT, Anseth KS, Bowman CN. Polymer 2000;41(11):3993–4004.
[29] Peppas NA, Hilt JZ, Khademhosseini A, Langer R. Adv Mater 2006;18(11):1345–60.
[30] Lin CC, Metters AT. Adv Drug Deliv Rev 2006;58(12–13):1379–408.
[31] English AE, Tanaka T, Edelman ER. Polymer 1998;39(24):5893–7.
[32] English AE, Tanaka T, Edelman ER. Macromolecules 1998;31(6):1989–95.
[33] Tabata Y, Ikada Y. Adv Drug Deliv Rev 1998;31(3):287–301.
[34] Tabata Y, Yamamoto M, Ikada Y. Pure Appl Chem 1998;70(6):1277–82.
[35] Tabata Y, Ikada Y. Biomaterials 1999;20(22):2169–75.
[36] Fukunaka Y, Iwanaga K, Morimoto K, Kakemi M, Tabata Y. J Controlled Release 2002;80(1–3):333–43.
[37] Kasahara H, Tanaka E, Fukuyama N, Sato E, Sakamoto H, Tabata Y, et al. Am Coll Cardiol 2003;41(6):1056–62.
[38] Kushibiki T, Tomoshige R, Fukunaka Y, Kakemi M, Tabata Y. J. Controlled Release 2003;90(2):207–16.
[39] Einerson NJ, Stevens KR, Kao WJ. Biomaterials 2003;24(3):509–23.
[40] Young S, Wong M, Tabata Y, Mikos AG. J. Controlled Release 2005;109(1-3):256–74.
[41] Nagarkar RP, Schneider JP. Synthesis and primary characterization of self-assembled peptide-based hydrogels. In: Gazit E, Nussinov R, editors. Methods in molecular biology. Nanostructure design: methods and protocols, vol 474. Totowa: Humana Press; 2008. p. 61–77.
[42] Ofner III CM, Bubnis WA. Pharm Res 1996;13(12):1821–7.
[43] Strauss G, Gibson SM. Food Hydrocolloids 2004;18(1):81–9.
[44] Ch Yao, Liu B, Ch Chang, Hsu S, Chen Y. Mater Chem Phys 2004;83(2–3):204–8.
[45] Mwangi JW, Ofner III CM. Int J Pharm 2004;278(2):319–27.
[46] Cao N, Fu Y, He J. Food Hydrocolloids 2007;21(4):575–84.
[47] Lien SM, Li WT, Huang TJ. Mater Sci Eng C 2008;28(1):36–46.
[48] Hoare TR, Kohane DS. Polymer 2008;49(8):1993–2007.
[49] Ross-Murphy SB. Polymer 1982;33(12):2622–6.
[50] Djabourov M, Lechaire JP, Gaill F. Biorheology 1993;30(3–4):191–205.
[51] Ito A, Mase A, Takizawa Y, Shinkai M, Honda H, Hata K, et al. Biosci Biochem 2003;95(2):196–9.

[52] Yung CW, Wu LQ, Tullman JA, Payne GF, Bentley WE, Barbari TA. J Biomed Mater Res Part A 2007;83(4):1039–46.
[53] Flory PJ. Principles of polymer chemistry. 9th ed. London: Cornell University Press; 1975 (chapter XI).
[54] Erman B, Mark JE. The molecular basis of rubberlike elasticity. In: Mark JE, Erman B, Eirich FR, editors. Science and technology of rubber. New York: Academic Press; 1994. p. 189–210.
[55] Erman B, Mark JE. Structures and properties of rubberlike networks. 1st ed. Oxford: Oxford University Press; 1997 (chapter 2).
[56] Mark JE, Erman B. Molecular aspects of rubber elasticity. In: Stepto RFT, editor. Polymer networks. New York: Blackie Academic & Professional; 1998. p. 215–42.
[57] Shibayama M, Tanaka T. Adv Polym Sci 1993;109:1–62.
[58] Eastoe JE, Leach AA. Chemical constitution of gelatin. In: Ward AG, Courts A, editors. The science and technology of gelatin. New York: Academic Press; 1977. p. 73–107.
[59] Bigi A, Cojazzi G, Panzavolta S, Rubini K, Roveri N. Biomaterials 2001;22(8):763–8.
[60] Bigi A, Cojazzi G, Panzavolta S, Roveri N, Rubini K. Biomaterials 2002;23(24):4827–32.
[61] Bigi A, Panzavolta S, Rubini K. Biomaterials 2004;25(25):5675–80.
[62] Blatz PJ, Sharda SC, Tschoegl NW. Trans Soc Rheology 1974;18(1):145–61.
[63] Nelson DL, Cox MM. Lehninger principles of biochemistry. 3th ed. New York: W.H. Freeman and Company; 2000 (chapter 5).
[64] Piaggio MV, Peirotti MB, Deiber JA. Electrophoresis 2005;26(17):3232–46.
[65] Piaggio MV, Peirotti MB, Deiber JA. Electrophoresis 2007;28(20):3658–76.
[66] Piaggio MV, Peirotti MB, Deiber JA. Electrophoresis 2009;30(13):2328–36.
[67] Rubinstein M, Colby RH. Polymer physics. 1st ed. Oxford: Oxford University Press; 2004 (chapter 7).
[68] Seth BR. Second order effects in elasticity, plasticity and fluid mechanics. In: Reiner M, Abir D, editors. Applied mechanics. New York: Mc Millam; 1964. p. 162–72.
[69] Rubinstein M, Colby RH, Dobrynin AV, Joanny JF. Macromolecules 1996;29(1):398–406.
[70] Creighton TE. Proteins: structures and molecular properties. 2nd ed. New York: W.H. Freeman and Company; 1993 (chapter 5).
[71] Bahar I, Erbil HY, Baysal BM, Erman B. Macromolecules 1987;20(6):1353–6.
[72] Edgecombe S, Linse P. Macromolecules 2007;40(10):3868–75.
[73] Kovac J. Macromolecules 1978;11(2):362–5.
[74] Galli AJ, Brumage WH. J Chem Phys 1983;79(5):2411–8.
[75] Huang Y, Szleifer I, Peppas NA. Macromolecules 2002;35(4):1373–80.
[76] Russell WB, Saville DA, Schowalter WR. Colloidal dispersions. 1st ed. Cambridge: Cambridge University Press; 1989 (chapter 4).
[77] Dobrynin AV, Zhulina EB, Rubinstein M. Macromolecules 2001;34(3):627–39.
[78] Kamiyama Y, Israelachvili J. Macromolecules 1992;20(19):5081–8.
[79] Bowman WA, Rubinstein M, Tan JS. Macromolecules; 30(11):3262–3270.
[80] Dobrynin AV, Obukhov SP, Rubinstein M. Macromolecules 1999;32(17):5689–700.
[81] Watanabe T, Ito K, Alvarez-Lorenzo C, Grosberg AY, Tanaka T. J. Chem Phys 2001;115(3):1596–600.
[82] Jeon J, Dobrynin AV. Macromolecules 2005;38(12):5300–12.